Published in final edited form as:

Biotechnol Bioeng. 2020 May ; 117(5): 1584–1596. doi:10.1002/bit.27287.

Pulsed Electromagnetic Fields Promote Repair of Focal Articular Cartilage Defects with Engineered Osteochondral Constructs

Robert M. Stefani[1], **Sofia Barbosa**[1], **Andrea R. Tan**[1], **Stefania Setti**[2], **Aaron M. Stoker**[3], **Gerard A. Ateshian**[1], **Ruggero Cadossi**[2], **Gordana Vunjak-Novakovic**[1], **Roy K. Aaron**[4], **James L. Cook**[3], **J. Chloe Bulinski**[1], **Clark T. Hung**[1,*]

[1]Columbia University, New York, NY

[2]University of Missouri, Columbia, MO

[3]IGEA Clinical Biophysics, Carpi, Italy

[4]Brown University, Providence, RI

Abstract

Articular cartilage injuries are a common source of joint pain and dysfunction. We hypothesized that pulsed electromagnetic fields (PEMFs) would improve growth and healing of tissue engineered cartilage grafts in a time- and direction-dependent manner. PEMF stimulation of engineered cartilage constructs was first evaluated *in vitro* using passaged adult canine chondrocytes embedded in an agarose hydrogel scaffold. PEMF coils oriented parallel to the articular surface induced superior repair stiffness compared to both perpendicular PEMF ($p=0.026$) and control ($p=0.012$). This was correlated with increased GAG deposition in both parallel and perpendicular PEMF orientations compared to control ($p=0.010$ and 0.028, respectively). Following *in vitro* optimization, the potential clinical translation of PEMF was evaluated in a preliminary *in vivo* preclinical adult canine model. Engineered osteochondral constructs (∅ 6 mm x 6 mm thick, devitalized bone base) were cultured to maturity and implanted into focal defects created in the stifle (knee) joint. To assess expedited early repair, animals were assessed after a 3-month recovery period, with microfracture repairs serving as an additional clinical control. *In vivo,* PEMF led to a greater likelihood of normal chondrocyte (OR: 2.5, $p=0.051$) and proteoglycan (OR: 5.0, $p=0.013$) histological scores in engineered constructs. Interestingly, engineered constructs outperformed microfracture in clinical scoring, regardless of PEMF treatment ($p<0.05$). Overall, the studies provided evidence that PEMF stimulation enhanced

*Clark T. Hung, 351 Engineering Terrace Building, Mail Code 8904, 1210 Amsterdam Avenue, New York, NY 10027, Tel: (212) 854-6542, Fax: (212) 854-8725, cth6@columbia.edu.

Author contributions: All authors contributed significantly to the work reported in this manuscript. RMS and CTH designed the experiments. RMS, SB, ART, LRG, HMK, AMS, and JLC carried out the experiments and collected the data. SS prepared and calibrated the PEMF devices. GAA, RC, GVN, RKA, JLC, JCB, and CTH supervised and advised the work. RMS and CTH wrote the paper. All authors have read and approved the final submitted manuscript.

Competing interests: The funding sources had no role in the study design, data collection, data analysis, or in the preparation and submission of the manuscript. SS is an employee of and RC is an owner of IGEA Clinical Biophysics, who provided the PEMF coils used in these experiments. SS and RC did not play a role in data collection, analysis, or determining content of the manuscript. None of the remaining authors had a financial or personal relationship with organizations that could influence the work presented in this manuscript.

engineered cartilage growth and repair, demonstrating a potential low-cost, low-risk, non-invasive treatment modality for expediting early cartilage repair.

Keywords

Pulsed Electromagnetic Fields; Osteochondral Repair; Tissue Engineering

Introduction

Articular cartilage injuries are a common source of joint pain and dysfunction. It has been reported that approximately 60% of knee arthroscopies find chondral lesions, 67% of which can be categorized as focal defects (Widuchowski, Widuchowski, & Trzaska, 2007). Cartilage repair and restoration surgeries, such as microfracture (MF), osteochondral autograft transfer (OAT), osteochondral allograft (OCA), and cell-culture techniques (ie. autologous chondrocyte implantation) are each limited by a number of factors, including availability of graft tissue, donor site morbidity, and difficulty in matching size and surface contours (Bugbee, Pallante-Kichura, Görtz, Amiel, & Sah, 2016; Nover et al., 2015). In attempts to overcome some of these issues, a number of engineered cartilage technologies (e.g. MACI®) are progressing through the clinical pipeline (Iwasa, Engebretsen, Shima, & Ochi, 2009; Pietschmann et al., 2009). However, wider adoption of engineered cartilage technologies is hindered by economic factors as well as difficulty in recapitulating native properties.

Pulsed electromagnetic fields (PEMFs) hold potential as a low-cost, low-risk, non-invasive adjunctive therapy for improving cartilage repair. Historically, PEMFs have been used in a clinical setting to treat delayed unions of bone fractures (Becker, Spadaro, & Marino, 1977). More recently, clinical studies of PEMFs have shown improvements in subjective measures of clinical function and pain following anterior cruciate ligament (ACL) reconstruction, bone marrow-derived stem cell (BMSC) transplantation, matrix-assisted chondrocyte implantation (MACI®), microfracture, and chondroabrasion (Francesco Benazzo et al., 2008; Cadossi et al., 2014; Collarile, Sambri, Lullini, Cadossi, & Zorzi, 2018; Osti, Del Buono, & Maffulli, 2015; Zorzi, Dall'Oca, Cadossi, & Setti, 2007). However, while these initial clinical studies were promising, additional preclinical and mechanistic studies are required in order to support or oppose the regular use of PEMFs as an adjuvant strategy for cartilage repair rather than as a pain management tool (American Academy of Orthopaedic Surgeons Board of Directors, 2013; Bjordal et al., 2007; Gobbi, Lad, Petrera, & Karnatzikos, 2014).

In vitro experiments have shown that PEMFs increase chondrocyte proliferation and matrix production while also protecting against catabolic stimuli (Mattei et al., 2001; Ongaro et al., 2011; Vincenzi et al., 2013). Meanwhile, improved cartilage growth was observed in an *in vivo* rabbit model of bone marrow concentrate and scaffold-based repair (Francesca Veronesi et al., 2015). In an *in vivo* sheep model of autograft repair, PEMF led to increased concentrations TGFβ, a modulator of cartilage growth; however, histological cartilage scores were unaffected and clinical functional measures were not assessed (Franco Benazzo et al., 2008). Motivated by these results, we sought to optimize PEMF parameters

for improved cartilage repair using engineered osteochondral grafts, which are especially susceptible to impacts from sub-optimal implantation properties and pro-inflammatory cytokines (Djouad, Rackwitz, Song, Janjanin, & Tuan, 2009; Hunter & Levenston, 2004; Obradovic, Martin, Padera, et al., 2001; Spalazzi et al., 2008). We further speculated that inconsistent shielding and/or distortion of the induced electric field (Polk, 1991) caused by variable coil positioning and graft type may be a reason for inconsistent results for cartilage healing. Specifically, we hypothesized that 1) PEMFs will improve *in vitro* growth and integration of engineered cartilage grafts in an orientation-dependent manner, and 2) PEMFs will expedite cartilage healing leading to better outcomes using engineered cartilage (Fini et al., 2013).

In these studies, clinical stimulation parameters (Collarile et al., 2018; Gobbi et al., 2014; Zorzi et al., 2007) were used to investigate the effect of PEMFs on engineered canine cartilage. A preclinical canine model was selected for its similarities to humans in patellofemoral joint pathology and presentation of pain and discomfort via changes to gait (Bendele, 2001), which allowed both tissue-level analysis and clinically relevant functional analyses. We first assessed the effect of orientation (Study 1) of PEMF stimulation on engineered cartilage growth and integration, two often cited factors contributing to clinical graft failure (Hunter & Levenston, 2004; Obradovic, Martin, Freed, & Vunjak-Novakovic, 2001). Study 1 was conducted *in vitro*, to serve as a best-case scenario permitting the evaluation of the intrinsic response of engineered cartilage to PEMF stimulation. Then, a comprehensive analysis of tissue quality and functional outcomes was performed following an *in vivo* engineered osteochondral allograft or microfracture repair (Study 2). A 3-month end point was selected in order to match the normal length of stimulation for clinical pain management (Collarile et al., 2018; Osti et al., 2015; Zorzi et al., 2007) and also capture the effect on expedited graft repair. To the author's knowledge, PEMFs have not previously been investigated as a method for improving engineered cartilage growth and integration, with complementary functional analyses, in a preclinical animal model.

Methods

PEMF System

The PEMF generators were custom made and calibrated to recapitulate clinical parameters by IGEA Clinical Biophysics (Carpi, Italy). The system consisted of electromagnetic coils made of copper wire and placed in a signal generator. This created a 1.5 ± 0.2 mT magnitude pulse with a duration of 1.3 ms and frequency of 75 Hz, yielding a duty cycle of 0.10. The magnetic peak field intensity was measured by the Hall probe (HTD61–0608-05-T, F.W. Bell, Sypris Solutions, Louisville, KY) of a gaussmeter (Walker Scientific, Auburn Hills, MI, USA) with a reading sensitivity equal to 0.2%. The induced electric field was measured by a standard coil probe (50 turns, 0.5 cm internal diameter of the coil probe, 0.2 copper diameter). A digital oscilloscope was used to evaluate the temporal pattern of the signal (Le Croy, Chestnut Ridge, NY). The shape and impulse length of the produced signal were maintained constant. Modeling of the PEMF-induced electrical field was performed by means of COMSOL Multiphysics 5.4 software.

The *in vitro* study (Study 1) was performed in a plexiglass chamber consisting of two parallel coils, also known as a Helmholtz pair (Fig. 1A). The paired coils created a large region with uniform field, ideal for use with tissue culture plates. The *in vivo* portion (Study 2) was performed using a single electromagnetic coil, which was strapped to the cranial (anterior) portion of the canine stifle (knee) joint, allowing for unrestricted range of motion (Fig. 2C). Previous work has shown that PEMFs induce less than a 0.1°C temperature change both *in vivo* and *in vitro* (Fini et al., 2008; Varani et al., 2008), so it was not monitored in this study.

Formation of TE Cartilage Constructs

Articular cartilage was harvested from the stifle of adult dogs (N=4 joints) euthanized for unrelated purposes. Briefly, chondrocytes were isolated via collagenase digestion and cultured in high glucose Dulbecco's Modified Eagle's Medium (hgDMEM; ThermoFisher) supplemented with 10% fetal bovine serum (FBS; Atlanta Biologicals), 1 ng/ml transforming growth factor beta 1 (TGF-β1; ThermoFisher), 5 ng/ml fibroblast growth factor-2 (FGF-2; ThermoFisher), and 1% antibiotic/antimycotic (ThermoFisher) for two passages (P2), or approximately 8 population doublings (Alegre-Aguarón et al., 2014; Ng et al., 2010a). P2 cells were encapsulated in agarose (2% (w/v) Type VII Agarose, Sigma) to form cylindrical constructs with an initial composition of 30×10^6 cells/ml (Ng et al., 2010a). Constructs were cultured in serum-free chondrogenic medium consisting of hgDMEM supplemented with 1% insulin transferrin selenium (ITS+) premix (Sigma), 50 μg/ml L-proline (Sigma), 0.9 mM sodium pyruvate (Sigma), 10 ng/ml TGF-β3 (Life Technologies), 100 nM dexamethasone (Sigma), and 50 μg/ml ascorbic acid-2-phosphate (Sigma).

Study 1 (in vitro): Effect of PEMF Orientation on Engineered Cartilage Integration

Cartilage constructs were prepared (∅ 8 mm x 2.4 mm thick) and cultured to maturity (42 days). At maturity, constructs were sub-punched using a 3 mm biopsy punch (Integra Miltex). The 3 mm cores were then randomly re-inserted into each annulus to create an implant-defect model. The core-annulus units were placed in 1 of 3 conditions: PEMF stimulation with electromagnetic coils oriented either perpendicular (⊥ PEMF) or parallel (═ PEMF) to the construct surface and no-PEMF controls (CTL) (Fig. 1A–C). PEMF was applied for 8 hr/day, 7 days/week. CTL specimens were cultured in adjacent sham chambers. No detectable electromagnetic field in CTL chambers, as measured with a Tesla Meter (F.W. Bell).

Specimen biochemical properties were evaluated at 42 days (start of implantation) and 72 days (1-month post-implantation) (N=8–12). Integration of the core-annulus unit was evaluated using an indentation "push-out" test at the terminal time point (Fig. 1D–E). Briefly, an indenter was visually centered over the core before loading at a rate of 10 μm/sec (Lima et al., 2008; van de Breevaart Bravenboer et al., 2004). The stiffness (slope of linear portion of force-displacement curve; Fig. 1E, v.), failure load (maximum observed force; Fig. 1E, vi.), and energy to failure (area under the load-displacement curve to the peak load and normalized to interface area; Fig. 1E, vii.) were computed for each specimen. After the cores were separated from the annuli via this destructive mechanical testing, individual core/

annulus specimens were solubilized using proteinase K (MP Biomedicals) prior to being assayed for DNA, glycosaminoglycans (GAG), and collagen (COL) using the Picogreen Assay (Life Technologies), dimethylmethylene blue dye assay, and orthohydroxyproline (OHP) assay, respectively. Biochemical content was expressed as a percentage of construct wet weight (ww).

Study 2 (in vivo): Effect of PEMF in a Preclinical Model of Engineered Osteochondral Repair

Osteochondral grafts (∅ 6 mm x 6 mm thick) were prepared and cultured as previously described (Lima et al., 2008). Briefly, bovine trabecular bone cores (∅ 6 mm x 5 mm thick) were devitalized and then infused with 2% (w/v) Type VII Agarose containing P2 canine chondrocytes (30×10^6 cells/ml) to produce layered osteochondral constructs with a 1 mm gel-only region, 1 mm gel bone interface, and 4 mm bone-only. Constructs were pre-cultured until the cartilage layer reached maturity (42 days).

Animal studies were performed in accordance with institutional guidelines and protocols approved by the University of Missouri-Columbia Institutional Animal Care and Use Committee (IACUC #9167). Studies also complied with the US National Research Council's Guide for the Care and Use of Laboratory Animals, the US Public Health Service's Policy on Humane Care and Use of Laboratory Animals, and Guide for the Care and Use of Laboratory Animals. Purpose-bred adult mongrel dogs (0.9 ± 0.07 yr, 24.0 ± 1.78 kg, all female) were anesthetized and prepared for aseptic surgery of the right stifle. Briefly, 2 doses of cefazolin (antibiotic) were given perioperatively and 2 morphine intramuscular doses plus 2 doses of oral tramadol were given for pain management. Post-operatively, a soft padded bandage was kept on the operated right hindlimb for 1 week with oral cefpodoxime (antibiotic) for 10 days.

Mature allogenic osteochondral constructs (N=8 animals, N=3 grafts per animal) were press-fit into defects created using a 6 mm OATS® reamer with power pick (Fig. 2A, trochlear repair not shown). Specifically, one defect each was created in the trochlear groove (TG), femoral condyle-medial (FCM), and femoral condyle-lateral (FCL) of the stifle joint. A parallel set of repairs were performed in defects (∅ 6 mm x 1 mm thick) using the microfracture (power pick) technique (N=8 animals, N=3 repairs per joint) (Fig. 2B, trochlear repair not shown).

Starting on the first post-operative day, all animals were fitted with PEMF devices which were then worn for 6 hr/day, 7 days/week for 3 months. Coils were positioned to approximate a "parallel" orientation (Fig. 2C), and animals were allowed to move freely, as is standard practice in OCA procedures. The stimulation time was shortened from the 8 hr/day used for *in vitro* experiments to 6 hr/day for the *in vivo* study due to practical reasons. Half of the devices were active (+ or PEMF, N=4 animals per repair type) and the other half were sham control devices (- or CTL, N=4 animals per repair type).

Evaluation of Functional Outcomes and Tissue Quality

Animals were examined by a board-certified veterinary orthopedic surgeon (JLC) prior to performing surgical procedures. Clinical lameness (pre-surgery: 0), functional gait (pre-

surgery: 10), comfortable range of motion (CROM; pre-surgery: 107.9°; 95% CI, 107.3 to 108.4°), pain (pre-surgery: 0), effusion (pre-surgery: 0), and total pressure index (TPI; pre-surgery: 21.0%; 95% CI, 20.6 to 21.4%) were assessed both pre-surgery (T=0) and at the conclusion of the study period (T=3 months) (Bozynski et al., 2015).

At the terminal 3-month time point, animals were sacrificed and tissue harvested for histopathology assessment. Osteochondral repair units including adjacent cartilage and bone were collected, fixed in formalin, and stained with H&E, picrosirius red, and toluidine blue. Immunohistochemical staining was performed using collagen type II primary antibody (ab34712; Abcam) and DAB staining kit (ab64264; Abcam).

Changes to cartilage and subchondral bone were evaluated with a modified OARSI method (Cook et al., 2010). A modified OCA scoring system was used to evaluate quality and integration of the engineered osteochondral repairs (E. Y. Chang et al., 2014). All histological scoring was performed by two blinded reviewers, with higher values indicating greater degree of pathology.

Statistics

Data sets were tested for normality (Kolmogorov-Smirnov Test) and homogeneity (Bartlett's Test). When necessary, data was log-transformed to achieve normality. Outliers were found using Grubb's Test (α=0.05). For *in vitro* measurements, one-way ANOVA with Tukey post hoc test (α=0.05) was used. *In vivo* functional measures were compared using three-way ANOVA (repair type, PEMF, time) with time as a repeated measures factor and Tukey post-hoc test (α=0.05). These normally distributed data were presented as mean (95% Confidence Interval (95% CI)). Parametric analyses were performed using GraphPad Prism.

Modified OARSI scores and corresponding sub-scores were analyzed using a Generalized Linear Model. Specifically, data were fit to an ordinal multinomial probability distribution and cumulative logit link function with generalized estimating equations correction for repeated measures (location, scorer). The dependent (response) variable was the score (or sub-score) and the independent variables (predictors) were the categorical factors: repair type, PEMF, and/or repair location. Total OARSI scores were grouped into ordered categories for regression analysis in order to increase the number of observations per level of the dependent variable. Odds ratios (OR) and corresponding 95% CI were computed from the model's parameter estimates. OCA scores were evaluated using the Mann-Whitney test. Averages of non-normal datasets were presented as median (95% CI). Ordinal regression analyses were performed using SPSS. The results of a pilot study were used to determine the sample size needed in Study 2 to achieve at least 80% power with G*Power 3 (α=0.05) (Faul, Erdfelder, Lang, & Buchner, 2007).

Results

Finite Element Modeling of Electric Field Distribution

In the perpendicular PEMF coil orientation, the induced electric field was predicted to peak at opposite ends of the construct resulting in an irregular charge distribution on the outer surface (Fig. 3). The parallel PEMF coil orientation generated an electrical field

and consequent charge distribution peaking along the outer circumference of the cartilage construct. In this case, the field was symmetric with regards to the axis of the cylinder, generating a homogenous distribution.

Effect of PEMF on Repair of Mature Engineered Cartilage Model (Study 1)

Repair stiffness was significantly greater in the parallel PEMF orientation compared to CTL (3.1 vs. 2.4 N/mm; between-group difference, 0.73 N/mm; p=0.012) and compared to perpendicular PEMF (3.1 vs. 2.4 N/mm; between-group difference, 0.71 N/mm; p=0.026) (Fig. 4A). Additionally, there was a significant increase in failure load for the parallel PEMF orientation relative to CTL (Fig. 4B; 6.4 vs. 4.6 N; between-group difference, 1.7 N; p=0.017) and a nonsignificant increase in energy to failure (Fig. 4C; 310 vs. 197 J/m^2; between-group difference, 113 J/m^2; p=0.074) of the core-annulus unit.

DNA content was not significantly affected by PEMF treatment in either the construct cores or annuli (Fig. 5A). Annuli in the perpendicular PEMF group had significantly greater GAG content compared to CTL (5.6 vs. 4.0 %ww; between-group difference, 1.6 %ww; p=0.010) (Fig. 5B). GAG content was similarly increased in parallel PEMF compared to CTL (5.6 vs. 4.0 %ww; between-group difference, 1.6 %ww; p=0.028). While there were no significant differences in collagen content, perpendicular PEMF had a non-significant increase over parallel PEMF in the construct annuli (2.6 vs. 2.3 %ww; between-group difference, 0.3 %ww; p=0.12) (Fig. 5C).

In Vivo Functional Outcomes and Repair Quality (Study 2)

No infections or other adverse events were reported. PEMF-treated tissue-engineered osteochondral repairs (TE+) were approximately 70% less likely than those without PEMF (TE-) to have a worse (ie. higher) combined OARSI cartilage score (p=0.028) (Table 1). Specifically, TE+ samples were about 80% less likely to have greater proteoglycan pathology (p=0.013) and 60% less likely (p=0.051) to have greater chondrocyte pathology than TE-. This was reflected by toluidine blue staining, which was homogenously distributed in TE+ specimens and almost nonexistent in the superficial zone of TE- specimens (Fig. 6I–J).

There were no significant differences in repair quality at the graft-host junction (OCA score; p=0.31) (Table 2). However, H&E staining showed evidence of increased matrix fill-in for TE+ specimens compared to TE- (Fig. 6E–F).

In animals with tissue-engineered repairs, five out of six parameters (gait, CROM, TPI, pain, effusion) were not significantly changed from baseline (Table 3). At the same time, animals with microfracture repairs had significantly worse gait, CROM, and TPI scores. Tissue-engineered repairs led to less lameness than microfracture repairs in both no PEMF (1.3 vs. 2.0; between-group difference, 0.8; 95% CI, 0.01 to 1.5) and PEMF (1.3 vs. 2.0; between-group difference, 0.8; 95% CI, 0.01 to 1.5) conditions.

Histologically, tissue-engineered repairs had superior deposition of both GAG (Fig. 6I–L) and type II collagen (Fig. 6Q–T) compared to microfracture. There was not a significant effect of PEMF in determining overall cartilage pathology in microfracture (p=0.31).

However, picrosirius red staining intensity was more intense in non-PEMF groups for both tissue-engineered and microfracture repairs (Fig. 6M–P).

Discussion

The current studies examined the influence of PEMF on engineered cartilage fabricated from an agarose hydrogel with passaged canine chondrocytes. Agarose has long been used for chondrocyte culture and has been adopted as a biocompatible hydrogel scaffold in preclinical and clinical strategies for cartilage repair (Neves & Reis, 2016; Ng et al., 2010a; Selmi et al., 2008). Although not currently the standard of care, engineered cartilage repair techniques such as MACI® are increasingly gaining clinical acceptance. By improving strategies for integration and growth of tissue engineered cartilage, their full potential can be more fully realized.

Overall, we accept our hypothesis: PEMF improved growth and integration of engineered cartilage *in vitro* and improved *in vivo* healing. PEMF application led to increased GAG accumulation, and the parallel PEMF orientation was superior for integration strength (Study 1). Study 2 served the dual purpose of being a preliminary evaluation of PEMF for engineered cartilage repair *in vivo* while using *in vitro* findings to maximize chance of success. Engineered osteochondral grafts were pre-cultured for 42 days prior to implantation, ensuring that Young's modulus reached native values. Furthermore, the PEMF coil was placed on the canine stifle in a manner that approximated a parallel orientation.

When applied to mature engineered constructs *in vitro* (Study 1), PEMF had a robust effect on GAG deposition in the construct annuli (Fig. 5B), an effect that has previously been observed in mature cartilage explants (De Mattei et al., 2007; Ongaro et al., 2011). PEMF is known to increase FGF-2 (Tepper et al., 2004), which may have supported chondrocyte growth and survival in culture as well (Gibson, Lin, & Roque, 1997; Solchaga et al., 2005). No differences were observed in constructs cores, perhaps due to shielding or distortion of the EF by surrounding tissue (Petrofsky, 2008; Polk, 1991). This asymmetric effect highlights the need for consistent and well-defined PEMF protocols that take into account repair geometry, patient size, and position. However, as constructs were only implanted upon reaching native mechanical properties and PEMF did not decrease matrix accumulation within the core, we expect that this asymmetry would not negatively affect outcomes. Furthermore, finite element modeling showed that charge density was concentrated in the annuli for both PEMF orientations, near the repair junction (Fig. 3). However, since the dielectric properties of engineered cartilage are different than native cartilage (Gabriel, Lau, & Gabriel, 1996), even application of a uniform PEMF would not necessarily result in homogenous field as it is dependent on local tissue properties and their spatial homogeneity.

As core and annulus regions were analyzed *in toto*, it is possible that local variations in matrix synthesis were obscured. In the future, quantitative staining or local microscope-based material testing (Wang, Deng, Ateshian, & Hung, 2002) can be used to provide a more refined analysis. Nevertheless, PEMF orientation played a significant role in construct integration properties *in vitro*. Parallel PEMF outperformed perpendicular PEMF and CTL in terms of repair stiffness and ultimate failure load (Fig. 4A–B). This was potentially

a result of the more uniform charge density created by the parallel PEMF orientation, particularly at the core-annulus junction (Fig. 3). The slightly increased collagen content in the perpendicular group may have played a role as well, as it would counteract GAG-induced tissue swelling in the annulus thereby lowering the perceived integration strength.

Electric field (EF) -induced cell migration at the core-annulus interface was another potential contributor to improved graft integration in parallel PEMF specimens. Endogenous EFs are known to guide cell migration and proliferation in developing embryos (Robinson, 1985). Analogous to their role in development, direct current (DC) EF gradients of 1–10 V/cm guide cell migration during tissue regeneration in adult animals (Baker, Becker, & Spadaro, 1974; Lippiello, Chakkalakal, & Connolly, 1990; Nessler & Mass, 1987) and cause *in vitro* directed movement of musculoskeletal cells (P. G. Chao, Lu, Hung, Nicoll, & Bulinski, 2007; O'Connell et al., 2015; Sun, Wise, & Cho, 2004). The PEMF system used in this study created a relatively low intensity induced EF of approximately 0.071 mV/cm (Franco Benazzo et al., 2008), however chondrocyte migration has been observed with EFs as low as 0.8 V/cm *in vitro* (P.-H. G. Chao et al., 2000). The EF, which is perpendicular to the magnetic field lines (Fig. 1B), would be offset by 90° in the two orientations, likely causing different patterns of migration. Although migration behavior was not analyzed in this study, future experiments could examine this potential mechanism by tracking cell migration using labeling techniques.

In vivo (Study 2), PEMF-stimulated tissue-engineered repairs were significantly less likely than no PEMF controls to have cartilage pathology (OARSI cartilage score, Table 1). Specifically, PEMF-treated specimens were less likely to have proteoglycan- and chondrocyte- related pathology than control, which was also apparent from comparatively diffuse toluidine blue staining in the superficial zone of control specimens (Fig. 6I–J). Similar benefits to cartilage histological scores were observed in a guinea pig model of OA (F. Veronesi et al., 2014). This may have been due to increased TGFβ expression (Aaron & Ciombor, 2004) and chondrogenesis (Ciombor, Lester, Aaron, Neame, & Caterson, 2002; De Mattei et al., 2007; Ongaro et al., 2011), which is known to support growth of adult engineered cartilage and prevent de-differentiation (Alegre-Aguarón et al., 2014; Ng et al., 2010b).

In apparent agreement with the results of Study 1, tissue-engineered repair integration was improved by PEMF (OCA score, Table 2), although not significantly. H&E staining of the graft-host junction was more intense in PEMF-treated repairs (Fig. 6E–F). It is possible that these modest beneficial results at 3 months may be strengthened with increased duration of PEMF stimulation, as clinical studies of cartilage restoration typically follow-up for 2 years or longer (Collarile et al., 2018; Osti et al., 2015). It is also possible that a less robust effect was observed in OCA sub-scores due to minor variations in PEMF orientation introduced by knee flexion and repair location (TG vs. FCL or FCM). Although coil placement was selected to maximize parallel PEMF, we did not strictly control orientation *in vivo*; animals were allowed freedom of movement. This was supported by the orientation-independent benefits of PEMF on GAG synthesis (Study 1) combined with potential negative effects of joint immobilization (Magit, Wolff, Sutton, & Medvecky, 2007; Sherman et al., 2014).

Overall, disparate effects of PEMF were observed in microfracture and tissue-engineered osteochondral repairs. Microfracture repairs had a significantly increased likelihood of having subchondral bone pathology in PEMF compared to no PEMF control. The bone pathology presented as increased subchondral bone density, which was apparent in picrosirius red staining (Fig. 6O–P). This was likely driven in part by increased TGF-β1, BMP-2, and BMP-4 expression in osteoblasts (Bodamyali et al., 1998; Zhuang et al., 1997), as well as increased osteoblast proliferation and reduced osteoclast formation (K. Chang, Chang, Huang, Huang, & Shih, 2005; Otter, McLeod, & Rubin, 1998).

Increased bone growth has also been observed at the transplant-host junction of the subchondral bone in an *in vivo* autograft model (Franco Benazzo et al., 2008). While it was considered beneficial for early graft stabilization and preventing bone resorption, it is possible that PEMF dosage would need to be modified (i.e. lowered) in microfracture repairs to prevent this pathologic bone thickening. It is further speculated that due to tissue density and maturity, OCA repair, the current standard of care, would perhaps require an elevated PEMF dose in order to observe similar integrative benefits to cartilage that were seen in tissue-engineered constructs.

Microfracture repair tissue is often described as sub-optimal in quality (Mithoefer, McAdams, Williams, Kreuz, & Mandelbaum, 2009), and this was reflected in the improved functional outcome of engineered vs. microfracture repairs in Study 2. Microfracture had significantly worse scores at 3 months, compared to baseline, for gait, CROM, and TPI (Table 3). Meanwhile, these parameters were not significantly different from baseline in tissue-engineered groups, indicating a near absence of functional limitations. Engineered repairs outperformed microfracture in lameness score as well. This was likely due to superior cartilage tissue quality, as demonstrated by increased deposition of both GAG and type II collagen (Fig. 6).

To the authors knowledge, this is the first report of PEMF for improved engineered cartilage growth and integration, both *in vitro* and *in vivo*. Devitalized bone bases did not elicit an immunogenic response in biocompatibility tests (data not shown), and we anticipate that engineered cartilage is analogous to allogeneic cartilage allografts, which have been used clinically for decades and not thought to pose a significant immunogenic risk (Bugbee et al., 2016). This preliminary *in vivo* experiment was potentially limited by sample size, which was improved by creating multiple defects per knee. However, trends and significant between-group differences were observed for many of the outcome measures. While some success in alleviating pain has been reported in previous clinical PEMF studies, our preclinical model provides a valuable platform for optimizing focal defect repair protocols based on individual mechanisms of action. While the underlying signaling pathways mediating the observed PEMF response were beyond the scope of the current study, studies in the literature have implicated the adenosine receptors/signaling in FLS as well as chondrocytes (Varani et al., 2008; Vincenzi et al., 2013), intracellular calcium signaling (Pall, 2013; Zhuang et al., 1997), and potential modulation of the cell resting potential (Funk, 2018). Going forward, it will be important to evaluate these mechanisms in the current system and determine if benefits to growth translate to improved long-term clinical repairs.

Conclusions

Under the conditions of the current studies, including clinically relevant parameters associated with the IGEA device, our data demonstrates that applied PEMFs can enhance engineered cartilage repair through modulation of cartilage growth and healing. Using *in vitro* models (Study 1) and confirmatory *in vivo* models (Study 2) of cartilage restoration provide guidance for optimizing PEMF strategies to maximize clinical cartilage graft survival and function. Moving forward, we hypothesize that PEMF dosage can be further optimized by extending treatment duration, leading to better long-term clinical outcomes. Although not currently the standard of care, engineered cartilage repair techniques are increasingly gaining clinical acceptance. By improving strategies for preparation and implantation of tissue engineered cartilage, the full potential of tissue engineered constructs can be more fully realized.

Acknowledgments

Thank you to Chantelle Bozynski and Keiichi Kuroki for conducting histology and clinical scoring.

Funding: This work was supported by CDMRP W81XWH-14-1-0591, NIH AR061988, Johnson & Johnson Summer Research Fellowship (SB), and NYSTEM predoctoral fellowship (RMS). The PEMF units were generously provided by IGEA.

Grant Numbers: CDMRP W81XWH-14-1-0591, NIH AR061988, NYSTEM DOH01-C30291GG-3450000

References

Aaron RK, & Ciombor DM (2004). Pain in osteoarthritis. Medicine and Health, Rhode Island, 87(7), 205–209.

Alegre-Aguarón E, Sampat SR, Xiong JC, Colligan RM, Bulinski JC, Cook JL, … Hung CT (2014). Growth Factor Priming Differentially Modulates Components of the Extracellular Matrix Proteome in Chondrocytes and Synovium-Derived Stem Cells. PLOS ONE, 9(2), e88053. 10.1371/journal.pone.0088053

American Academy of Orthopaedic Surgeons Board of Directors. (2013). Treatment of osteoarthritis of the knee: Evidence-based guideline (2nd ed.). Retrieved from https://www.aaos.org/cc_files/aaosorg/research/guidelines/treatmentofosteoarthritisofthekneeguideline.pdf

Baker B, Becker RO, & Spadaro J. (1974). A study of electrochemical enhancement of articular cartilage repair. Clinical Orthopaedics and Related Research, (102), 251–267.

Becker RO, Spadaro JA, & Marino AA (1977). Clinical experiences with low intensity direct current stimulation of bone growth. Clinical Orthopaedics and Related Research, (124), 75–83. [PubMed: 304404]

Benazzo Francesco, Zanon G, Pederzini L, Modonesi F, Cardile C, Falez F, … Massari L. (2008). Effects of biophysical stimulation in patients undergoing arthroscopic reconstruction of anterior cruciate ligament: Prospective, randomized and double blind study. Knee Surgery, Sports Traumatology, Arthroscopy, 16(6), 595–601. 10.1007/s00167-008-0519-9

Benazzo Franco, Cadossi M, Cavani F, Fini M, Giavaresi G, Setti S, … Giardino R. (2008). Cartilage repair with osteochondral autografts in sheep: Effect of biophysical stimulation with pulsed electromagnetic fields. Journal of Orthopaedic Research, 26(5), 631–642. 10.1002/jor.20530 [PubMed: 18176941]

Bendele AM (2001). Animal models of osteoarthritis. J Musculoskel Neuron Interact, 1(4), 363–376.

Bjordal JM, Johnson MI, Lopes-Martins RAB, Bogen B, Chow R, & Ljunggren AE (2007). Short-term efficacy of physical interventions in osteoarthritic knee pain. A systematic review and meta-analysis of randomised placebo-controlled trials. BMC Musculoskeletal Disorders, 8, 51. 10.1186/1471-2474-8-51 [PubMed: 17587446]

Bodamyali T, Bhatt B, Hughes FJ, Winrow VR, Kanczler JM, Simon B, … Stevens CR (1998). Pulsed electromagnetic fields simultaneously induce osteogenesis and upregulate transcription of bone morphogenetic proteins 2 and 4 in rat osteoblasts in vitro. Biochemical and Biophysical Research Communications, 250(2), 458–461. 10.1006/bbrc.1998.9243 [PubMed: 9753652]

Bozynski CC, Kuroki K, Stannard JP, Smith PA, Stoker AM, Cook CR, & Cook JL (2015). Evaluation of Partial Transection versus Synovial Debridement of the ACL as Novel Canine Models for Management of ACL Injuries. The Journal of Knee Surgery, 28(5), 404–410. 10.1055/s-0035-1544975 [PubMed: 25635873]

Bugbee WD, Pallante-Kichura AL, Görtz S, Amiel D, & Sah R. (2016). Osteochondral allograft transplantation in cartilage repair: Graft storage paradigm, translational models, and clinical applications. Journal of Orthopaedic Research, 34(1), 31–38. 10.1002/jor.22998 [PubMed: 26234194]

Cadossi M, Buda RE, Ramponi L, Sambri A, Natali S, & Giannini S. (2014). Bone Marrow–derived Cells and Biophysical Stimulation for Talar Osteochondral Lesions: A Randomized Controlled Study. Foot & Ankle International, 35(10), 981–987. 10.1177/1071100714539660 [PubMed: 24917648]

Chang EY, Pallante-Kichura AL, Bae WC, Du J, Statum S, Wolfson T, … Chung CB (2014). Development of a Comprehensive Osteochondral Allograft MRI Scoring System (OCAMRISS) With Histopathologic, Micro–Computed Tomography, and Biomechanical Validation. CARTILAGE, 5(1), 16–27. 10.1177/1947603513514436 [PubMed: 24489999]

Chang K, Chang WH-S, Huang S, Huang S, & Shih C. (2005). Pulsed electromagnetic fields stimulation affects osteoclast formation by modulation of osteoprotegerin, RANK ligand and macrophage colony-stimulating facto. Journal of Orthopaedic Research, 23(6), 1308–1314. 10.1016/j.orthres.2005.03.012.1100230611 [PubMed: 15913941]

Chao PG, Lu HH, Hung CT, Nicoll SB, & Bulinski JC (2007). Effects of Applied DC Electric Field on Ligament Fibroblast Migration and Wound Healing. Connective Tissue Research, 48(4), 188–197. 10.1080/03008200701424451 [PubMed: 17653975]

Chao P-HG, Roy R, Mauck RL, Liu W, Valhmu WB, & Hung CT (2000). Chondrocyte Translocation Response to Direct Current Electric Fields. Journal of Biomechanical Engineering, 122(3), 261–267. 10.1115/1.429661 [PubMed: 10923294]

Ciombor DM, Lester G, Aaron RK, Neame P, & Caterson B. (2002). Low frequency EMF regulates chondrocyte differentiation and expression of matrix proteins. Journal of Orthopaedic Research: Official Publication of the Orthopaedic Research Society, 20(1), 40–50. 10.1016/S0736-0266(01)00071-7 [PubMed: 11853089]

Collarile M, Sambri A, Lullini G, Cadossi M, & Zorzi C. (2018). Biophysical stimulation improves clinical results of matrix-assisted autologous chondrocyte implantation in the treatment of chondral lesions of the knee. Knee Surgery, Sports Traumatology, Arthroscopy, 26(4), 1223–1229. 10.1007/s00167-017-4605-8

Cook JL, Kuroki K, Visco D, Pelletier J-P, Schulz L, & Lafeber FPJG (2010). The OARSI histopathology initiative – recommendations for histological assessments of osteoarthritis in the dog. Osteoarthritis and Cartilage, 18, S66–S79. 10.1016/j.joca.2010.04.017 [PubMed: 20864024]

De Mattei M, Fini M, Setti S, Ongaro A, Gemmati D, Stabellini G, … Caruso A. (2007). Proteoglycan synthesis in bovine articular cartilage explants exposed to different low-frequency low-energy pulsed electromagnetic fields. Osteoarthritis and Cartilage, 15(2), 163–168. 10.1016/j.joca.2006.06.019 [PubMed: 16905341]

Djouad F, Rackwitz L, Song Y, Janjanin S, & Tuan RS (2009). ERK1/2 Activation Induced by Inflammatory Cytokines Compromises Effective Host Tissue Integration of Engineered Cartilage. Tissue Engineering Part A, 15(10), 2825–2835. 10.1089/ten.tea.2008.0663 [PubMed: 19243242]

Faul F, Erdfelder E, Lang A-G, & Buchner A. (2007). G*Power 3: A flexible statistical power analysis program for the social, behavioral, and biomedical sciences. Behavior Research Methods, 39(2), 175–191. 10.3758/BF03193146 [PubMed: 17695343]

Fini M, Pagani S, Giavaresi G, De Mattei M, Ongaro A, Varani K, … Cadossi M. (2013). Functional Tissue Engineering in Articular Cartilage Repair: Is There a Role for Electromagnetic Biophysical Stimulation? Tissue Engineering Part B: Reviews, 19(4), 353–367. 10.1089/ten.teb.2012.0501 [PubMed: 23339690]

Fini M, Torricelli P, Giavaresi G, Aldini NN, Cavani F, Setti S, … Giardino R. (2008). Effect of pulsed electromagnetic field stimulation on knee cartilage, subchondral and epyphiseal trabecular bone of aged Dunkin Hartley guinea pigs. Biomedicine & Pharmacotherapy, 62(10), 709–715. 10.1016/j.biopha.2007.03.001 [PubMed: 17459652]

Funk RH (2018). Coupling of pulsed electromagnetic fields (PEMF). Am J Transl Res, 10(5), 1260–1272. [PubMed: 29887943]

Gabriel S, Lau RW, & Gabriel C. (1996). The dielectric properties of biological tissues: II. Measurements in the frequency range 10 Hz to 20 GHz. Physics in Medicine and Biology, 41(11), 2251–2269. 10.1088/0031-9155/41/11/002 [PubMed: 8938025]

Gibson G, Lin D-L, & Roque M. (1997). Apoptosis of Terminally Differentiated Chondrocytes in Culture | Elsevier Enhanced Reader. Experimental Cell Research, (233), 372–382. 10.1006/excr.1997.3576 [PubMed: 9194499]

Gobbi A, Lad D, Petrera M, & Karnatzikos G. (2014). Symptomatic Early Osteoarthritis of the Knee Treated With Pulsed Electromagnetic Fields: Two-Year Follow-up. CARTILAGE, 5(2), 78–85. 10.1177/1947603513515904 [PubMed: 26069687]

Hunter CJ, & Levenston ME (2004). Maturation and integration of tissue-engineered cartilages within an in vitro defect repair model. Tissue Engineering, 10(5–6), 736–746. 10.1089/1076327041348310 [PubMed: 15265290]

Iwasa J, Engebretsen L, Shima Y, & Ochi M. (2009). Clinical application of scaffolds for cartilage tissue engineering. Knee Surgery, Sports Traumatology, Arthroscopy, 17(6), 561–577. 10.1007/s00167-008-0663-2

Lima EG, Grace Chao P, Ateshian GA, Bal BS, Cook JL, Vunjak-Novakovic G, & Hung CT (2008). The effect of devitalized trabecular bone on the formation of osteochondral tissue-engineered constructs. Biomaterials, 29(32), 4292–4299. 10.1016/j.biomaterials.2008.07.018 [PubMed: 18718655]

Lippiello L, Chakkalakal D, & Connolly JF (1990). Pulsing direct current-induced repair of articular cartilage in rabbit osteochondral defects. Journal of Orthopaedic Research: Official Publication of the Orthopaedic Research Society, 8(2), 266–275. 10.1002/jor.1100080216 [PubMed: 2303960]

Magit D, Wolff A, Sutton K, & Medvecky MJ (2007). Arthrofibrosis of the Knee. JAAOS - Journal of the American Academy of Orthopaedic Surgeons, 15(11), 682.

Mattei MD, Caruso A, Pezzetti F, Pellati A, Stabellini G, Sollazzo V, & Traina GC (2001). Effects of Pulsed Electromagnetic Fields on Human Articular Chondrocyte Proliferation. Connective Tissue Research, 42(4), 269–279. 10.3109/03008200109016841 [PubMed: 11913771]

Mithoefer K, McAdams T, Williams RJ, Kreuz PC, & Mandelbaum BR (2009). Clinical Efficacy of the Microfracture Technique for Articular Cartilage Repair in the Knee: An Evidence-Based Systematic Analysis. The American Journal of Sports Medicine, 37(10), 2053–2063. 10.1177/0363546508328414 [PubMed: 19251676]

Nessler JP, & Mass DP (1987). Direct-current electrical stimulation of tendon healing in vitro. Clinical Orthopaedics and Related Research, (217), 303–312.

Neves NM, & Reis RL (2016). Biomaterials from Nature for Advanced Devices and Therapies. John Wiley & Sons.

Ng KW, Lima EG, Bian L, O'Conor CJ, Jayabalan PS, Stoker AM, … Hung CT (2010a). Passaged Adult Chondrocytes Can Form Engineered Cartilage with Functional Mechanical Properties: A Canine Model. Tissue Engineering. Part A, 16(3), 1041–1051. 10.1089/ten.tea.2009.0581 [PubMed: 19845465]

Ng KW, Lima EG, Bian L, O'Conor CJ, Jayabalan PS, Stoker AM, … Hung CT (2010b). Passaged Adult Chondrocytes Can Form Engineered Cartilage with Functional Mechanical Properties: A Canine Model. Tissue Engineering. Part A, 16(3), 1041–1051. 10.1089/ten.tea.2009.0581 [PubMed: 19845465]

Nover AB, Stefani RM, Lee SL, Ateshian GA, Stoker AM, Cook JL, & Hung CT (2015). Long-term storage and preservation of tissue engineered articular cartilage. Journal of Orthopaedic Research, 34(1), 141–148. 10.1002/jor.23034 [PubMed: 26296185]

Obradovic B, Martin I, Freed LE, & Vunjak-Novakovic G. (2001). Bioreactor studies of natural and tissue engineered cartilage. Ortopedia, Traumatologia, Rehabilitacja, 3(2), 181–189.

Obradovic B, Martin I, Padera RF, Treppo S, Freed LE, & Vunjak-Navakovic G. (2001). Integration of engineered cartilage. Journal of Orthopaedic Research, 19(6), 1089–1097. 10.1016/S0736-0266(01)00030-4 [PubMed: 11781010]

O'Connell GD, Tan AR, Cui V, Bulinski JC, Cook JL, Attur M, … Hung CT (2015). Human chondrocyte migration behaviour to guide the development of engineered cartilage. Journal of Tissue Engineering and Regenerative Medicine, n/a-n/a. 10.1002/term.1988

Ongaro A, Pellati A, Masieri FF, Caruso A, Setti S, Cadossi R, … De Mattei M. (2011). Chondroprotective effects of pulsed electromagnetic fields on human cartilage explants. Bioelectromagnetics, 32(7), 543–551. 10.1002/bem.20663 [PubMed: 21412809]

Osti L, Del Buono A, & Maffulli N. (2015). Application of pulsed electromagnetic fields after microfractures to the knee: A mid-term study. International Orthopaedics, 39(7), 1289–1294. 10.1007/s00264-014-2627-0 [PubMed: 25876224]

Otter MW, McLeod KJ, & Rubin CT (1998). Effects of Electromagnetic Fields in Experimental Fracture Repair: Clinical Orthopaedics and Related Research, 355S, S90–S104. 10.1097/00003086-199810001-00011

Pall ML (2013). Electromagnetic fields act *via* activation of voltage-gated calcium channels to produce beneficial or adverse effects. Journal of Cellular and Molecular Medicine, 17(8), 958–965. 10.1111/jcmm.12088 [PubMed: 23802593]

Petrofsky J. (2008). The effect of the subcutaneous fat on the transfer of current through skin and into muscle. Medical Engineering & Physics, 30(9), 1168–1176. 10.1016/j.medengphy.2008.02.009 [PubMed: 18400550]

Pietschmann MF, Horng A, Niethammer T, Pagenstert I, Sievers B, Jansson V, … Müller PE (2009). Cell quality affects clinical outcome after MACI procedure for cartilage injury of the knee. Knee Surgery, Sports Traumatology, Arthroscopy, 17(11), 1305–1311. 10.1007/s00167-009-0828-7

Polk C. (1991). Biological effects of low-level low-frequency electric and magnetic fields. IEEE Transactions on Education, 34(3), 243–249. 10.1109/13.85082

Robinson KR (1985). The responses of cells to electrical fields: A review. The Journal of Cell Biology, 101(6), 2023–2027. [PubMed: 3905820]

Selmi TAS, Verdonk P, Chambat P, Dubrana F, Potel J-F, Barnouin L, & Neyret P. (2008). Autologous chondrocyte implantation in a novel alginate-agarose hydrogel: OUTCOME AT TWO YEARS. The Journal of Bone and Joint Surgery. British Volume, 90-B(5), 597–604. 10.1302/0301-620X.90B5.20360

Sherman SL, Garrity J, Bauer K, Cook J, Stannard J, & Bugbee W. (2014). Fresh Osteochondral Allograft Transplantation for the Knee: Current Concepts. JAAOS - Journal of the American Academy of Orthopaedic Surgeons, 22(2), 121. 10.5435/JAAOS-22-03-199

Solchaga LA, Penick K, Porter JD, Goldberg VM, Caplan AI, & Welter JF (2005). FGF-2 enhances the mitotic and chondrogenic potentials of human adult bone marrow-derived mesenchymal stem cells. Journal of Cellular Physiology, 203(2), 398–409. 10.1002/jcp.20238 [PubMed: 15521064]

Spalazzi JP, Dagher E, Doty SB, Guo XE, Rodeo SA, & Lu HH (2008). In vivo evaluation of a multiphased scaffold designed for orthopaedic interface tissue engineering and soft tissue-to-bone integration. Journal of Biomedical Materials Research Part A, 86A(1), 1–12. 10.1002/jbm.a.32073

Sun S, Wise J, & Cho M. (2004). Human Fibroblast Migration in Three-Dimensional Collagen Gel in Response to Noninvasive Electrical Stimulus. I. Characterization of Induced Three-Dimensional Cell Movement. Tissue Engineering, 10(9–10), 1548–1557. 10.1089/ten.2004.10.1548 [PubMed: 15588414]

Tepper OM, Callaghan MJ, Chang EI, Galiano RD, Bhatt KA, Baharestani S, … Gurtner GC (2004). Electromagnetic fields increase in vitro and in vivo angiogenesis through endothelial release of FGF-2. FASEB Journal: Official Publication of the Federation of American Societies for Experimental Biology, 18(11), 1231–1233. 10.1096/fj.03-0847fje [PubMed: 15208265]

van de Breevaart Bravenboer J, In der Maur CD, Bos PK, Feenstra L, Verhaar JA, Weinans H, & van Osch GJ (2004). Improved cartilage integration and interfacial strength after enzymatic treatment in a cartilage transplantation model. Arthritis Res Ther, 6(5), R469. 10.1186/ar1216

Varani K, De Mattei M, Vincenzi F, Gessi S, Merighi S, Pellati A, … Borea PA (2008). Characterization of adenosine receptors in bovine chondrocytes and fibroblast-like synoviocytes

exposed to low frequency low energy pulsed electromagnetic fields. Osteoarthritis and Cartilage, 16(3), 292–304. 10.1016/j.joca.2007.07.004 [PubMed: 17698373]

Veronesi F, Torricelli P, Giavaresi G, Sartori M, Cavani F, Setti S, … Fini M. (2014). In vivo effect of two different pulsed electromagnetic field frequencies on osteoarthritis. Journal of Orthopaedic Research, 32(5), 677–685. 10.1002/jor.22584 [PubMed: 24501089]

Veronesi Francesca, Cadossi M, Giavaresi G, Martini L, Setti S, Buda R, … Fini M. (2015). Pulsed electromagnetic fields combined with a collagenous scaffold and bone marrow concentrate enhance osteochondral regeneration: An in vivo study. BMC Musculoskeletal Disorders, 16, 233. 10.1186/s12891-015-0683-2 [PubMed: 26328626]

Vincenzi F, Targa M, Corciulo C, Gessi S, Merighi S, Setti S, … Varani K. (2013). Pulsed Electromagnetic Fields Increased the Anti-Inflammatory Effect of A2A and A3 Adenosine Receptors in Human T/C-28a2 Chondrocytes and hFOB 1.19 Osteoblasts. PLoS ONE, 8(5). 10.1371/journal.pone.0065561

Wang CC-B, Deng J-M, Ateshian GA, & Hung CT (2002). An automated approach for direct measurement of two-dimensional strain distributions within articular cartilage under unconfined compression. Journal of Biomechanical Engineering, 124(5), 557–567. 10.1115/1.1503795 [PubMed: 12405599]

Widuchowski W, Widuchowski J, & Trzaska T. (2007). Articular cartilage defects: Study of 25,124 knee arthroscopies. The Knee, 14(3), 177–182. 10.1016/j.knee.2007.02.001 [PubMed: 17428666]

Zhuang H, Wang W, Seldes RM, Tahernia AD, Fan H, & Brighton CT (1997). Electrical stimulation induces the level of TGF-beta1 mRNA in osteoblastic cells by a mechanism involving calcium/calmodulin pathway. Biochemical and Biophysical Research Communications, 237(2), 225–229. 10.1006/bbrc.1997.7118 [PubMed: 9268690]

Zorzi C, Dall'Oca C, Cadossi R, & Setti S. (2007). Effects of pulsed electromagnetic fields on patients' recovery after arthroscopic surgery: Prospective, randomized and double-blind study. Knee Surgery, Sports Traumatology, Arthroscopy, 15(7), 830–834. 10.1007/s00167-007-0298-8

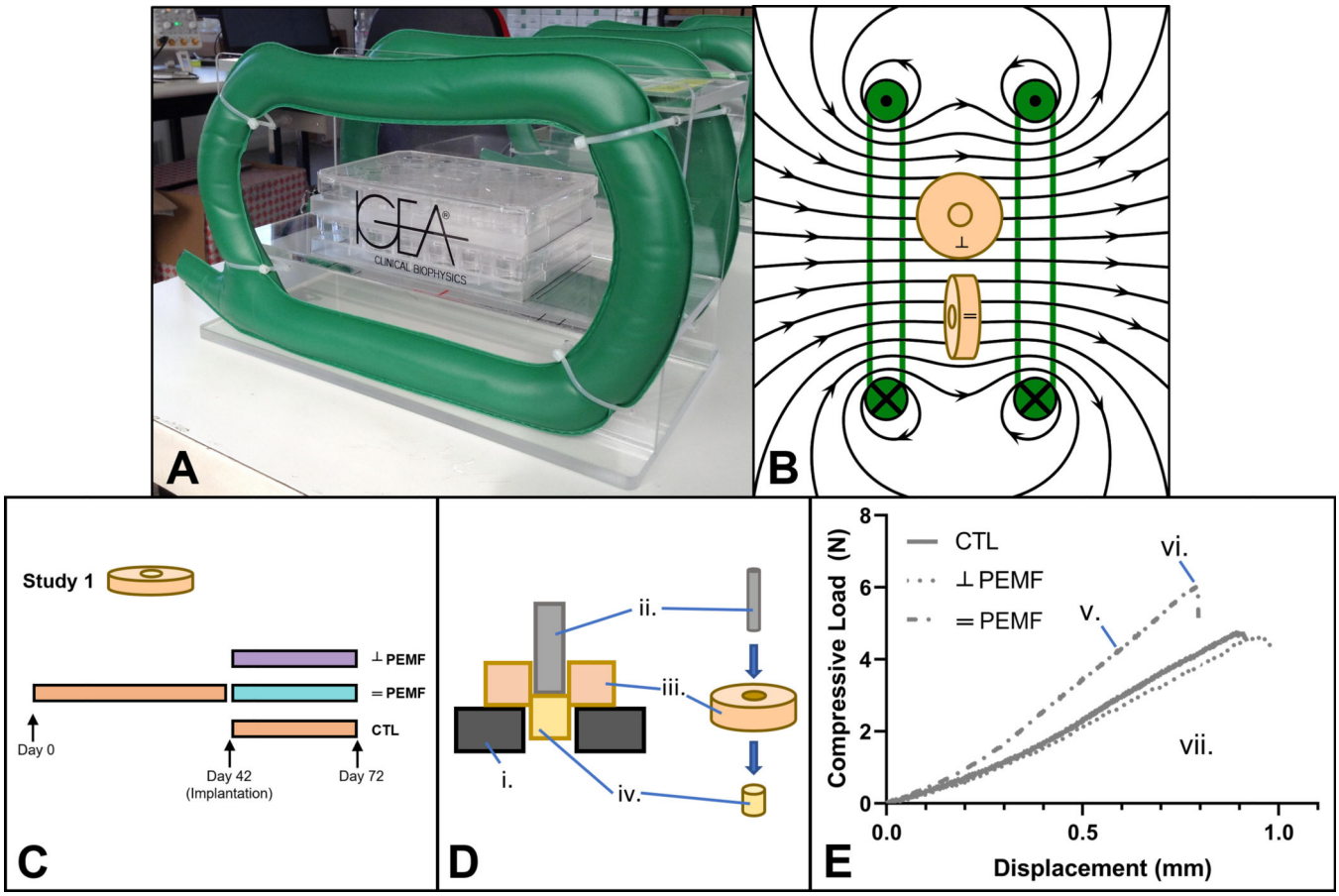

Figure 1.

Study 1 Schematic. **(A)** *In vitro* PEMF chamber consisting of two electromagnetic coils (green) created a uniform magnetic field in the culture area; **(B)** Magnetic field lines (modified from commons.wikimedia.org, labeled for reuse) with engineered constructs in perpendicular (⊥) or parallel (═) orientations; **(C)** Specimens were pre-cultured for 42 days and then sub-cored, re-implanted, and stimulated with either perpendicular (⊥) or parallel (═) orientation or no PEMF (CTL) for an additional 1 month; **(D)** Schematic of push-out testing of engineered core/annulus units (Study 1) showing side view and deconstructed oblique view with construct holder (i.), indenter (ii.), construct annulus (iii.), and construct core (iv.); **(E)** Representative load-displacement curves from push-out tests for perpendicular, parallel, and no PEMF groups (Study 1).

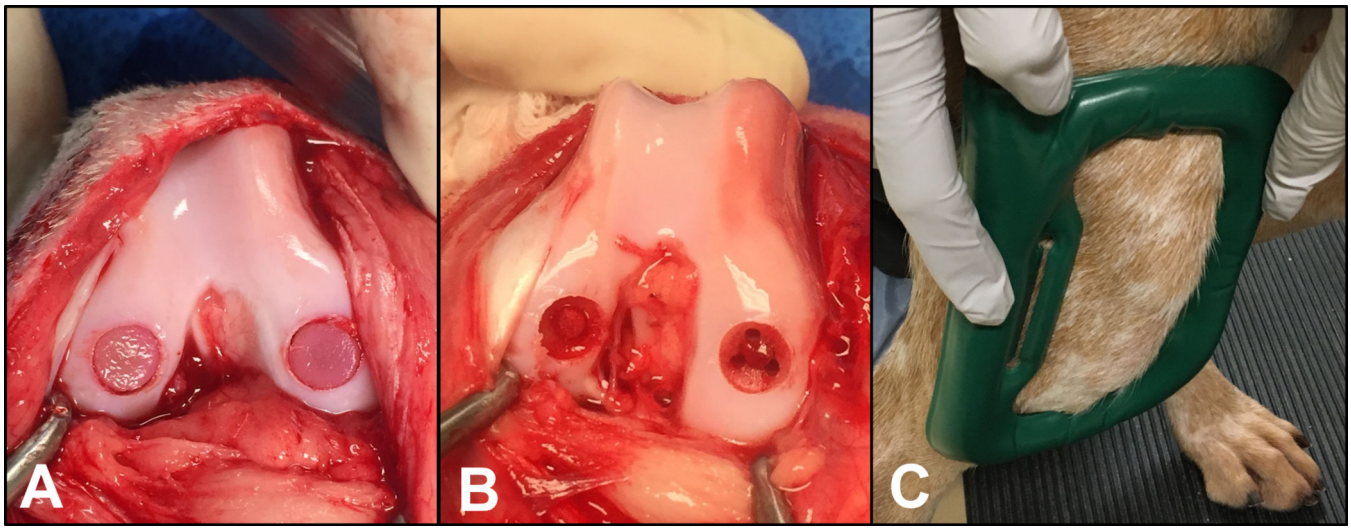

Figure 2.

Study 2 Schematic. **(A)** Two engineered osteochondral grafts (out of a total of 3 per joint, trochlear repair not shown) were implanted in the femoral condyles (Study 2); **(B)** Two microfracture procedures (total of 3 per joint, trochlear defect not shown) in the femoral condyles (Study 2); **(C)** Single electromagnetic coil (green) used for *in vivo* pilot allowed full range of motion (Study 2).

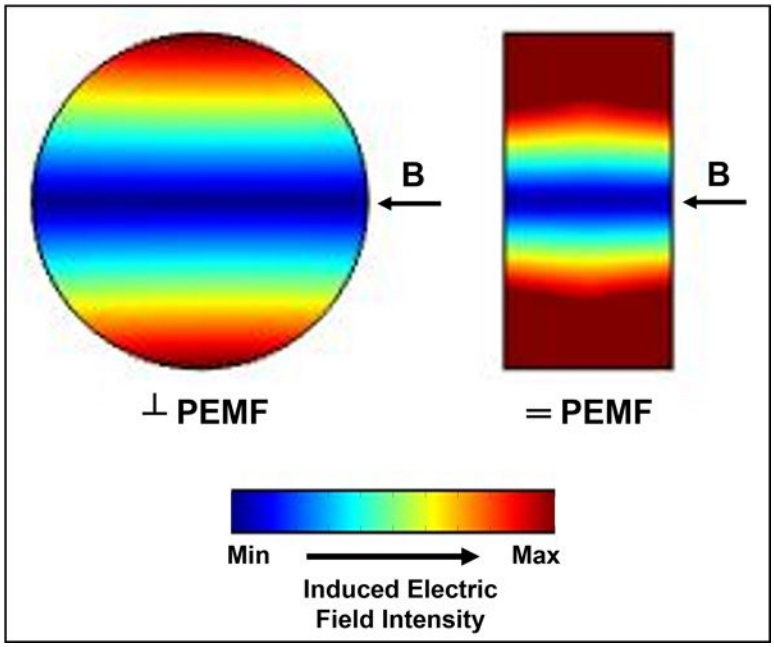

Figure 3.

Finite element analysis showing relative charge distribution within engineered cartilage constructs subjected to perpendicular and parallel PEMF orientations *in vitro*.

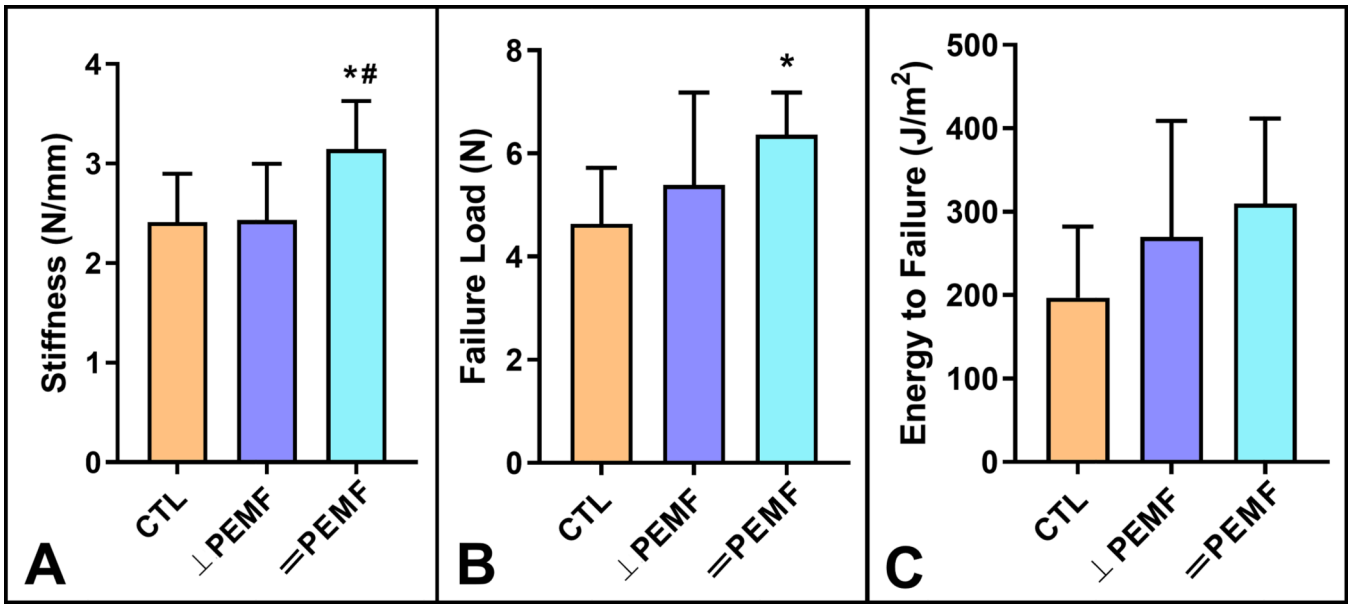

Figure 4.

Mechanical properties of core-annulus repairs in Study 1. **(A)** Stiffness (N/mm) was determined from the slope of the load-displacement curve, **(B)** failure load (N) from the peak load, and **(C)** energy to failure (J/m^2) from the area under the curve normalized to interface area. Each parameter was enhanced in the parallel (═PEMF) orientation relative to no PEMF (CTL); *$p<0.05$ compared to CTL, #$p<0.05$ compared to ⊥PEMF.

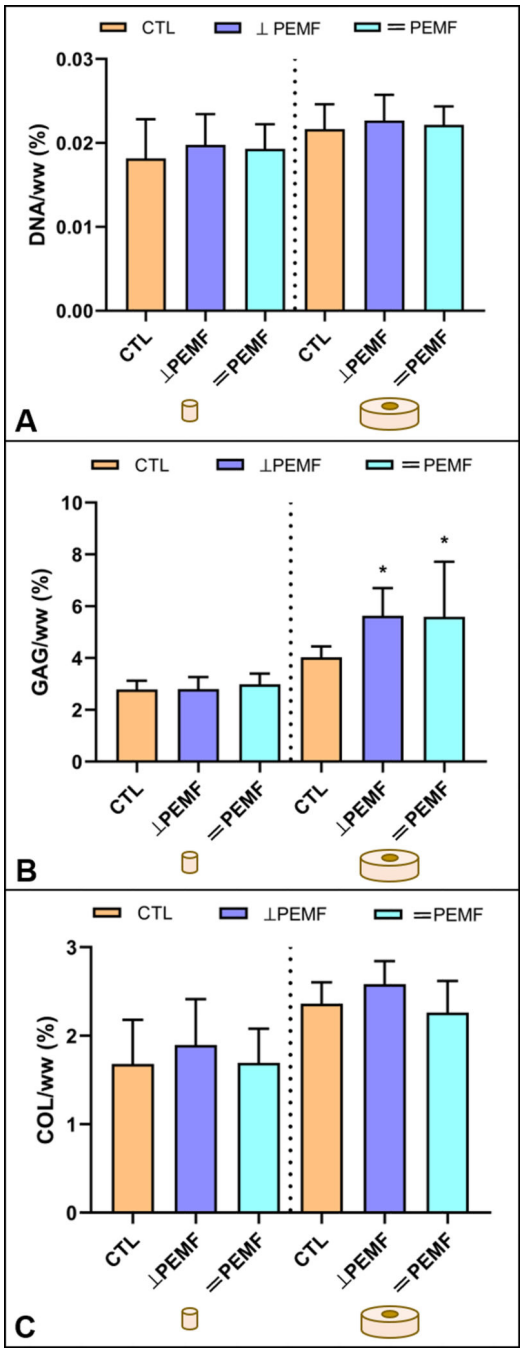

Figure 5.

Biochemical properties of engineered constructs in Study 1. **(A)** DNA/ww, **(B)** GAG/ww, and **(C)** COL/ww for the engineered construct cores (left) and annuli (right) in perpendicular (⊥) and parallel (═) PEMF groups compared to no PEMF (CTL) (Study 1); *p<0.05 compared to CTL.

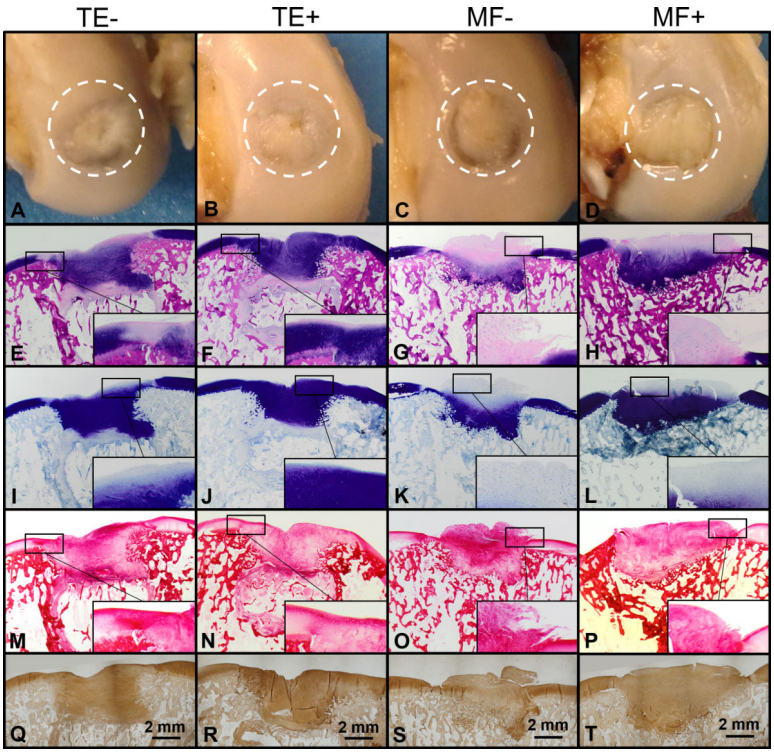

Figure 6.

Representative gross morphology **(A-D)**, H&E **(E-H)**, toluidine blue **(I-L)**, picrosirius red **(M-P)**, and type II collagen immunohistochemistry **(Q-T)** of TE- (ID 90-FCM; A, E, I, M, Q), TE+ (ID 101-FCM; B, F, J, N, R), MF- (ID 105-FCM; C, G, K, O, S), and MF+ (ID 110-FCM; D, H, L, P, T) at 3-month time point (Study 2); Tissue-engineered osteochondral repairs without PEMF (TE-) and with PEMF (TE+); microfracture repairs without PEMF (MF-) and with PEMF (MF+).

Table 1.

OARSI cartilage scores (Study 2)

	Median (95% CI)			Median (95% CI)		
Measurement	**TE-**	**TE+**	**Odds Ratio (95% CI)**	**MF-**	**MF+**	**Odds Ratio (95% CI)**
OARSI (Cartilage, combined)	19 (14 to 20)	18.5 (12 to 19)	0.3 (0.1 to 0.9) *	16 (13 to 19)	16.5 (15 to 20)	1.8 (0.6 to 5.7)
Structure	4 (2 to 4)	4 (1 to 4)	0.7 (0.2 to 2.0)	3.5 (2 to 4)	3 (2 to 4)	0.9 (0.2 to 3.6)
Chondrocytes	4 (2 to 4)	3.5 (1 to 4)	0.4 (0.1 to 1.0)	3 (2 to 4)	3 (2 to 4)	0.9 (0.2 to 4.5)
Proteoglycans	3 (2 to 4)	3 (1 to 3)	0.2 (0.1 to 0.7) *	3 (3 to 3)	3 (3 to 4)	0.8 (0.1 to 5.0)
Collagen	3 (3 to 3)	3 (3 to 3)	N/A	3 (3 to 3)	3 (3 to 3)	N/A
Tidemark	2 (2 to 2)	2 (2 to 2)	N/A	2 (2 to 2)	2 (2 to 2)	N/A
Bone	3 (3 to 3)	3 (3 to 3)	N/A	2 (1 to 3)	3 (3 to 3)	55.3 (9.4 to 326) ****

TE-, tissue-engineered osteochondral repairs without PEMF; TE+, tissue-engineered osteochondral repairs with PEMF; MF-, microfracture repairs without PEMF; MF+, microfracture repairs with PEMF

* $p<0.05$

**** $p<0.0001$

Table 2.

OC TE graft-host junction scores (Study 2).

	Median (95% CI)	
Measurement	**TE-**	**TE+**
OCA (Total)	7 (6 to 8)	6 (5 to 8)
Fill	2 (2 to 2)	2 (2 to 2)
Edge Integration	1 (1 to 1)	1 (0 to 2)
Surface Congruity	2 (1 to 2)	1 (0 to 2)
Fibrosis	1 (1 to 2)	1 (1 to 1)
Inflammation	1 (1 to 1)	1 (1 to 1)

TE-, tissue-engineered osteochondral repairs without PEMF; TE+, tissue-engineered osteochondral repairs with PEMF

Table 3.

Change in clinical function scores from baseline and between-group difference in change for gait, comfortable range of motion (CROM), total pressure index (TPI), lameness, pain, and effusion (Study 2)

	Mean (95% CI)			Mean (95% CI)			Mean (95% CI)	
	TE (Change from Baseline)		Difference in Change (TE- vs. TE+)	MF (Change from Baseline)		Difference in Change (MF- vs. MF+)	Difference in Change (TE- vs. MF-)	Difference in Change (TE+ vs. MF+)
Measurement	**TE-**	**TE+**		**MF-**	**MF+**			
Gait	−1.5 (−3.6 to 0.6)	−1.7 (−3.8 to 0.4)	−0.2 (−2.7 to 2.4)	−2.9 (−5.0 to −0.8) **	−3.9 (−5.9 to −1.8) ***	−0.9 (−3.4 to 1.6)	−1.4 (−3.9 to 1.1)	−2.2 (−4.7 to 0.3)
CROM	−7.5 (−20.2 to 5.2)	−10.8 (−23.4 to 1.9)	−3.3 (−18.4 to 11.9)	−17.5 (−30.2 to −4.8) **	−23.8 (−36.4 to −11.1) ***	−6.3 (−21.4 to 8.9)	−10.0 (−25.2 to 5.2)	−13.0 (−28.2 to 2.2)
TPI	−2.8 (−6.7 to 1.2)	−2.1 (−6.1 to 1.8)	0.7 (−4.1 to 5.4)	−4.4 (−8.4 to 0.5) *	−6.0 (−9.9 to −2.1) **	−1.6 (−6.3 to 3.1)	−1.7 (−6.4 to 3.1)	−3.9 (−8.6 to 0.8)
Lameness	1.3 (0.6 to 1.9) ***	1.3 (0.6 to 1.9) ***	0.0 (−0.7 to 0.7)	2.0 (1.4 to 2.6) ****	2.0 (1.4 to 2.6) ****	0.0 (−0.7 to 0.7)	0.8 (0.01 to 1.5) *	0.8 (0.01 to 1.5) *
Pain	1.3 (−0.6 to 3.2)	1.1 (−0.8 to 3.0)	−0.2 (−2.5 to 2.1)	1.5 (−0.5 to 3.4)	2.6 (0.7 to 4.5) **	1.2 (−1.1 to 3.5)	0.2 (−2.1 to 2.4)	1.6 (−0.7 to 3.8)
Effusion	1.3 (−1.7 to 4.3)	1.7 (−1.3 to 4.7)	0.5 (−3.1 to 4.0)	3.8 (0.8 to 6.8) **	2.6 (−0.4 to 5.5)	−1.2 (−4.8 to 2.3)	2.5 (−1.1 to 6.1)	0.8 (−2.7 to 4.4)

TE-, tissue-engineered osteochondral repairs without PEMF; TE+, tissue-engineered osteochondral repairs with PEMF; MF-, microfracture repairs without PEMF; MF+, microfracture repairs with PEMF

* p<0.05

** p<0.01

*** p<0.001

**** p<0.0001